CALCULATION OF FLOW PAST RECTANGULAR WINGS AND THEIR COMBINATIONS IN SUBSONIC FLOW USING A DISCRETE VORTEX SCHEME

N. F. Vorob'ev and G. N. Shashkina

UDC 533.69

For wings with a small aspect ratio, end effects greatly affect the aerodynamic characteristics. Separation of the flow from the edges of the wing leads to the formation of complex vortical configurations above and beyond the wing. The effect of separation phenomena can be taken into account within the framework of an ideal fluid [1, 2]. The method of discrete vortices is an efficient method for calculating flows in the plane near wings with a complicated shape, taking into account free vortex formations [3]. A discrete vortex scheme, which permits modeling different conditions of separation of the vortex sheet from the edges of a wing, was proposed in [4, 5]. Variation of the parameter K introduced therein, in the range $0 \leqslant K \leqslant 1$ corresponds to modeling the intensity of a separating vortex sheet (K = 0 corresponds to flow without separation; K = 1 is the limiting case of complete separation, corresponding to the scheme in [3]). The strong effect of the parameter K on aerodynamic characteristics of wings is noted in [4, 5] for triangular wings.

In this paper, we present calculations of the degree to which the parameter K affects the aerodynamic characteristics of rectangular (in the plane) wings, as well as methodical investigations of the effect of separate working parameters and separate elements of the free vortex sheet on the overall aerodynamic characteristics of wings. The flow past combinations of rectangular wings with small extension is calculated and the pattern of vortex structures and load distribution on wings are shown. The results of calculations of the normal force factors C_n and of the pitching moment m_z are compared with available experimental data. A scheme is proposed for modeling the rolling up of the vortex sheet into two vortex filaments at some distance beyond the wing; the "descent" of the filaments is established numerically.

The load on the wing is calculated using Bernoulli's integral and the velocity field induced by the entire vortical system, modeling the wing and the free vortex sheet.

1. The problem of nonviscous flow past wings with finite span is characterized by the following geometrical parameters: the wing aspect ratio λ; shape of the wing in the plane P; shape of the wing surface, on which the conditions for separation of the vortex sheet from the edges K depends; and parameters of the oncoming flow: the Mach number M and angle of attack α. In solving the problem using a discrete vortex scheme, the following computational parameters appear: number of computational points on the wing $N_X \times N_Z$; fixed accuracy of the calculations ε; choice of distance at which the flow parameters are considered to coincide with the parameters of the unperturbed flow x_∞. Sometimes [6], when the iteration process does not converge, a computational radius R is introduced, which could affect the results of the calculation [4]. In this work, the calculations were performed without introducing a computational radius.

The determining computational parameter in the scheme being examined is the parameter $N_X \times N_Z$, related to the available on-line computer memory and the time for performing the calculation. An accuracy of 1-2% with respect to C_n and 4% with respect to m_z was obtained in the calculations of flow past separate rectangular waves λ = 0.5, 1.0, and 2.0 performed below. The same accuracy was not obtained in calculations of combinations of wings due to the inadequate on-line memory of the BÉSM-6 computer.

For flow past a wing, the vortex sheet, shed by the edges of the wing, assumes a form with which the vortex lines coincide with the stream lines. It is possible to compute the degree to which the separate elements of the vortex sheet affect the aerodynamic characteristics of wings. It was established in [4] in calculations of flow past triangular wings $1 \leqslant \lambda \leqslant 7$ that the form of the vortex wake, beginning with $x_\infty = 2$, has practically no effect on the aerodynamic characteristics of a wing and on the form of the free current sheet above

Novosibirsk. Translated from Zhurnal Prikladnoi Mekhaniki i Tekhnicheskoi Fiziki, No. 2, pp. 91-98, March-April, 1983. Original article submitted June 25, 1982.

 0021-8944/83/2402-0220$07.50

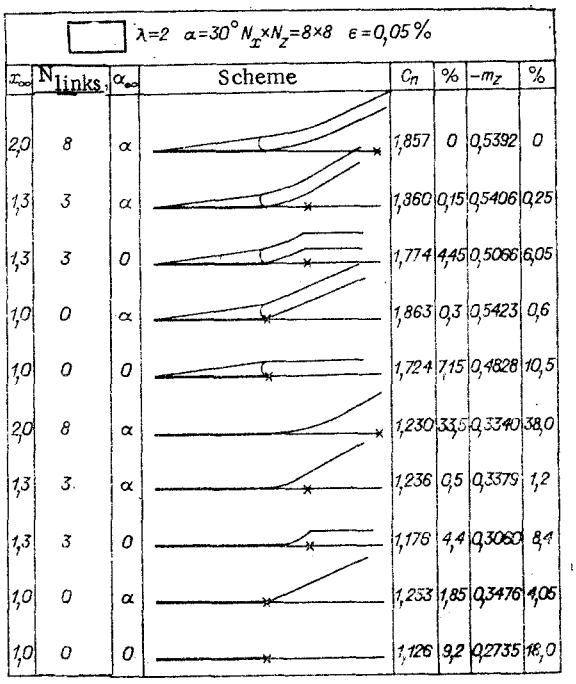

x_∞	N_{links}	α_∞	Scheme	C_n	%	$-m_z$	%
2,0	8	α		1,857	0	0,5392	0
1,3	3	α		1,860	0,15	0,5406	0,25
1,3	3	0		1,774	4,45	0,5066	6,05
1,0	0	α		1,863	0,3	0,5423	0,6
1,0	0	0		1,724	7,15	0,4828	10,5
2,0	8	α		1,230	33,5	0,3340	38,0
1,3	3	α		1,236	0,5	0,3379	1,2
1,3	3	0		1,176	4,4	0,3060	8,4
1,0	0	α		1,233	1,85	0,3476	4,05
1,0	0	0		1,126	9,2	0,2735	16,0

Fig. 1

the wing and it may be assumed that the vortex lines coincide beginning with $x_\infty = 2$ with the direction of the unperturbed flow.

The results of calculations of values of C_n and m_z for different forms of the vortex sheet and the difference between these values in percent and the most complete calculations are shown in Fig. 1 for a rectangular wing $\lambda = 2$ with $\alpha = 30°$ for $N_x \times N_z = 8 \times 8$. The reference calculation used for the separation flow past the wing is a calculation in which the vortex lines line up in the process of iteration along the stream lines, and beginning with $x_\infty = 2$ they assume the orientation $\alpha_\infty = \alpha$; the number of free links in each vortex line from the section $x = 1$, corresponding to the back edge of the wing, to the section $x_\infty = 2$ in this case is $N_{links} = 8$. As is evident from the computed data presented in Fig. 1, the form of the sheet beyond the wing has little effect on the magnitude of the aerodynamic characteristics. If it is assumed that immediately behind the wing the vortex lines assume the orientation of the velocity at infinity ($x_\infty = 1$, $N_{links} = 0$, $\alpha_\infty = \alpha$), then the difference between the values of C_n and m_z from their reference values does not exceed 1%. The difference between the results of calculations of C_n using the scheme of separation flow past the wing for parameters $x_\infty = 2$ and 1.3 does not exceed 1% (the calculations were performed with $\varepsilon = 0.05\%$). But, since the accuracy of the calculations, depending on the parameter $N_x \times N_z = 8 \times 8$, is of the order of 1% for this case, it is sufficient to perform calculations for $x_\infty = 1.3$.

The weak effect of the form of the trailing sheet on the overall characteristics of wings should be used to reduce the computational time required to reach a steady state with given accuracy. The time to reach the steady state strongly depends on the value of x_∞ and the number of links in the free vortex sheet in the wake behind the wing. Thus, for a rectangular wing $\lambda = 2$ with $\alpha = 15°$ for $N_x \times N_z = 8 \times 8$, $\varepsilon = 0.01\%$, 100 min of BÉSM-6 time are required for $x_\infty = 2$ and 40 min for $x_\infty = 1.3$.

Another parameter that permits saving computer time is the fixed accuracy of the calculations ε. Thus, for the same wing $\lambda = 2$, $\alpha = 15°$, $N_x \times N_z = 8 \times 8$, $x_\infty = 1.3$, the computer time is reduced to 20 min for $\varepsilon = 0.5\%$.

Figure 1 also shows calculations for flow past the lateral edges of the wing without separation when the vortex sheet is shed only by the trailing edge, for different forms of the trailing sheet. The reference calculation is the calculation in which the form of the sheet is aligned during the iteration process ($x_\infty = 2$, $N_{links} = 8$, $\alpha_\infty = \alpha$). All cases of separationless flow examined in Fig. 1 compare within a few percent with the reference calculation. The reference case of a separationless flow, in which only the form of the trailing edge of the sheet is taken into account, is itself compared with the reference case of

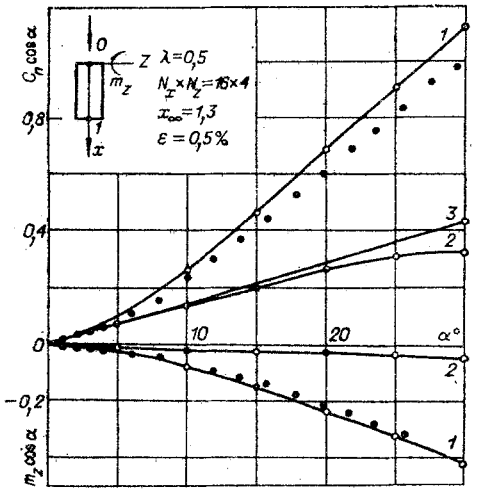

Fig. 2

separation flow in which the form of the trailing and lateral sheets are included. As is evident from the data presented in Fig. 1, taking into account the form of the trailing vortex sheet for a rectangular wing $\lambda = 2$ with $\alpha = 30°$ compared with the linear theory, when the vortex sheet beyond the wing is a continuation of the wing surface ($x_\infty = 1$, $N_{links} = 0$, $\alpha_\infty = 0$) gives a difference of 9% with respect to C_n and 18% with respect to m_z.

The vortex sheet shed from the lateral edges of the wing has the largest effect on the aerodynamic characteristics of the wing. The difference between the calculations including only the form of the trailing sheet and the calculations including the form of the lateral and trailing sheets is 33% with respect to C_n and 38% with respect to m_z for a wing with $\lambda = 2$. For wings with aspect ratio $\lambda < 2$, this difference will be greater. Thus, for a wing $\lambda = 2$ with $\alpha = 30°$ the difference with respect to C_n between the calculation based on the linear theory, when the trailing vortex sheet lies in the plane of the wing, and the calculation taking into account the form of the lateral and trailing sheets is 42% (33% + 9%), but with the same angle of attack $\alpha = 30°$, this difference for a wing with $\lambda = 1$ is 55% while for a wing with $\lambda = 0.5$, it is already 70%.

2. Calculations of the force factor normal to the surface of the wing C_n and the moment factor of this force relative to the front edge of the wing m_z are presented as a function of the attack angle α for rectangular wings with aspect ratio $\lambda = 0.5$, 1, and 2.

Figure 2 presents the values of $C_n \cos\alpha$ and $m_z \cos\alpha$ for aspect ratio $\lambda = 0.5$. Curve 1 corresponds to a calculation which includes complete shedding of the lateral vortex sheet ($K = 1$). Curve 2 corresponds to calculations using the linear theory ($x_\infty = 1$, $N_{links} = 0$, $\alpha_\infty = 0$). Curve 3 is a straight line drawn through the origin of coordinates and the value of the force factor for the resultant of the forces $C_R = C_n/\cos\alpha$ acting on the wing, calculated according to the linear theory with $\alpha = 30°$.

Figure 2 also shows the experimental results [7] obtained while testing a flat rectangular wing with $\lambda = 0.5$, relative to a thickness of 1.2%. As expected, the experimental results lie between the results of the linear theory of the separationless flow past the lateral edges ($K = 0$) and the results for complete separation ($K = 1$). The intensity of the vortex sheet, shed from the lateral edges, depends on the form of the end sections of the wing. This dependence is weaker for thin wings; for such wings, a flow close to the complete separation regime ($K = 1$) is realized. In Fig. 2, the experimental points are close to the computed curve, corresponding to $K = 1$. Such a coincidence of computed and experimental values is also observed for thin rectangular plates with aspect ratios $\lambda = 1$, $\lambda = 2$. A regime without separation of the flow from the front edge is realized up to attack angles close to 25° only for plates with $\lambda = 1$, while for plates with $\lambda = 2$, it is realized up to attack angles close to 15°. After this, the behavior of the computed dependences $C_n(\alpha)$ and $m_z(\alpha)$ differs from the experimental dependences since the computational scheme examined does not include separation from the front edge.

The aerodynamic characteristics of a combination of two rectangular wings with different aspect ratios, having identical chords and situated in the same plane at a distance of 3

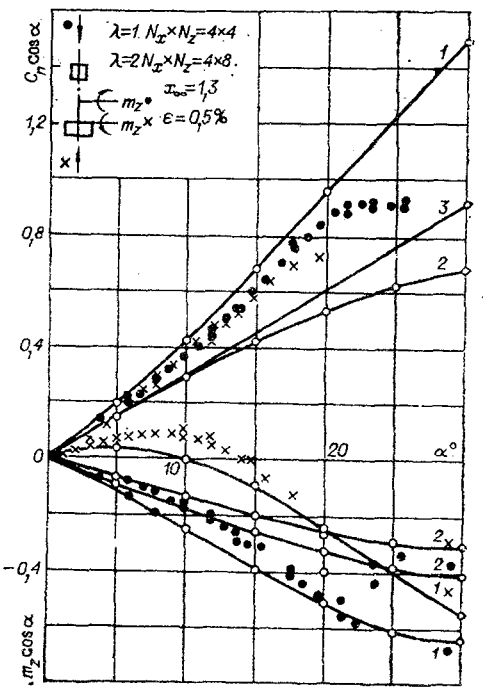

Fig. 3

chords, were calculated: 1) $\lambda = 1$, $\lambda = 2$; 2) $\lambda = 2$, $\lambda = 1$; 3) $\lambda = 2$, $\lambda = 2$.

In the calculations, the separation into cells was made so that there were $\lambda = 1$ $N_X \times N_Z = 4 \times 4 = 16$ cells on the wing with $\lambda = 1$ and $N_X \times N_Z = 4 \times 8 = 32$ cells on the wing with $\lambda = 2$. The distance between the front chord of the first and the rear chord of the second wing was taken as the distance unit. The length of the projections of segments of free vortex lines on the x axis equals 0.05. The free vortex lines are aligned by the method of iteration to $x_\infty = 1.3$, and then assume the orientation $\alpha_\infty = \alpha$. With this quite rough grid on the wings, the average accuracy of the calculations in tandem is estimated to be 4% for C_n and 12% for m_z.

Figure 3 presents the results of calculations of $C_n \cos\alpha$ and $m_z \cos\alpha$ as a function of the angle of attack α for tandem configurations $\lambda = 1$, $\lambda = 2$ and $\lambda = 2$, $\lambda = 1$. The same figure presents the results of experiments [7] on plates with relative thickness 1.2%. The line 1 corresponds to calculations taking into account shedding of the vortex sheet from the lateral edges of both wings according to the complete separation scheme (K = 1); line 2 corresponds to calculations using the linear theory; and, line 3 is a straight line drawn through the origin of coordinates and the value $C_R = C_n/\cos\alpha$, calculated according to the linear theory at $\alpha = 30°$. The moment is calculated relative to the line passing through the center of the distance between the wings for the tandem $\lambda = 1$, $\lambda = 2$ and relative to the rear edge of the front wing for the tandem $\lambda = 2$, $\lambda = 1$. In all cases, the moment is referred to the chord of the wing (the chords of both wings are identical). As is evident from the graphs presented, the computed quantities C_n, taking into account shedding of the vortex sheet from the lateral edges according to the complete separation scheme (K = 1) up to the onset of separation of flow from the front edges at large angles of attack ($\alpha \approx 15$-$20°$) give, just as in the case of isolated wings, the upper asymptote of the experimental results.

In performing the experiments on wings with different shape in the plane and on tandem wing combinations, it was found that the theorem of flow reversibility for C_n at large angles of attack is satisfied [7]. Figure 3 shows the results for the tandem $\lambda = 1$, $\lambda = 2$ (experimental results are shown by the dots) and for the tandem $\lambda = 2$, $\lambda = 1$ (experimental results are shown by cross marks). The experimental results for C_n for the cases $\lambda = 1$, $\lambda = 2$ and $\lambda = 2$, $\lambda = 1$ practically coincide up to angles of attack of 16° — up to the onset of separation from the front edge on the wing $\lambda = 2$. The calculations for the cases $\lambda = 1$, $\lambda = 2$ and $\lambda = 2$, $\lambda = 1$ for C_n up to angles $\alpha \leqslant 20°$ coincide with accuracy up to the graphs presented ($\leqslant 2\%$); in Fig. 3, they are indicated by the same curves 1-3 for both cases.

The reversibility theorem for the moment characteristics is not satisfied. The moment

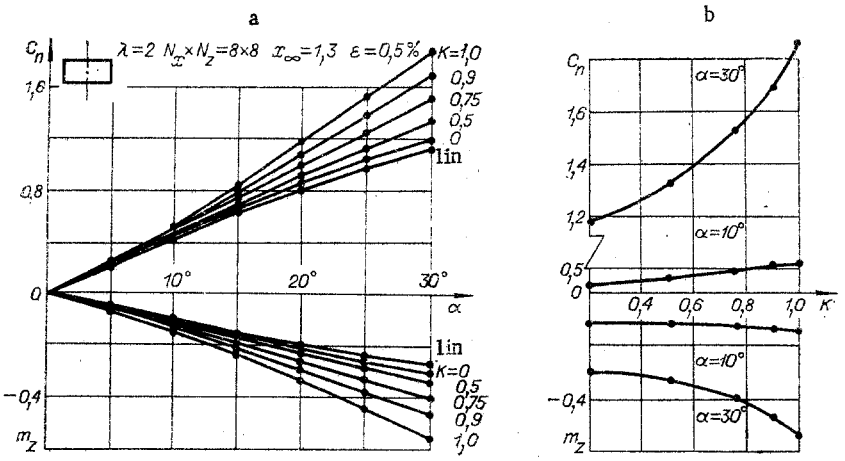

Fig. 4

characteristics for $\lambda = 1$, $\lambda = 2$ and $\lambda = 2$, $\lambda = 1$ differ so strongly that in order to show the results for $\lambda = 1$, $\lambda = 2$ on the same graph as the result for $\lambda = 2$, $\lambda = 1$, it is necessary to take the moment for $\lambda = 1$, $\lambda = 2$ relative to the axis passing through the center of the distance between the wings, while for $\lambda = 2$, $\lambda = 1$ the moment is taken relative to the axis passing through the rear edge of the front wing.

The qualitative agreement between the experimental values of $m_z(\alpha)$ and the computed values obtained taking into account the shedding of the vortex sheet from the lateral edges of the wings should be noted. The tandem case $\lambda = 1$, $\lambda = 2$ is shown by curve 1 in Fig. 3 with the dots and the tandem case $\lambda = 2$, $\lambda = 1$ is shown by curve 1 in Fig. 3 with the cross marks. Calculations of $m_z(\alpha)$ within the framework of the linear theory for the tandem configuration agree poorly with the experimental values (see curve 2 with the dots for the tandem $\lambda = 1$, $\lambda = 2$; curve 2 with the cross marks for the tandem $\lambda = 2$, $\lambda = 1$). The dependences $m_z(\alpha)$ computed within the framework of the linear theory for the tandem $\lambda = 2$, $\lambda = 2$ differ qualitatively from the experimental dependences.

3. Calculations of the normal force factor C_n and the pitching moment factor relative to the front edge m_z are presented as a function of the angle of attack α for a rectangular wing $\lambda = 2$ with different values of the parameter K, characterizing the intensity of the vortex sheet shed from the lateral edges. In Fig. 4a, curves K = 1 correspond to the scheme with complete separation from the lateral edges. Curves K = 0 correspond to separationless flow past the lateral edges when the trailing vortex sheet is aligned along the stream lines and at infinity the sheet is oriented along the unperturbed flow. Curves marked with "lin" correspond to the linear flow past the wing (separationless flow past the lateral edges; the trailing sheet beyond the wing lies in the plane of the wing).

As already noted, for large angles of attack, the overall characteristics calculated according to the complete separation scheme differ considerably from the overall characteristics calculated according to the linear scheme. For $\alpha = 30°$, the calculations using the linear theory differ from calculations with K = 1 by 39% for C_n and 50% for m_z.

Figure 4b shows the dependences $C_n = C_n(K)$ and $m_z = m_z(K)$ for two values: $\alpha = 10°$ and $\alpha = 30°$. The dependences are linear for $\alpha = 10°$ and nonlinear for $\alpha = 30°$.

4. According to the so-called nonlinear vortex scheme of the wing, vortex lines leaving the edges behave like free vortex lines forming a vortex sheet. The vortex sheet rolls under and remains, according to the calculations using the adopted scheme, a continuous vortex sheet at large distances beyond the wing.

Under real flight conditions, a vortex wake is observed behind the aircraft, which degenerates quite rapidly into two vortex filaments, whose interaction leads to the descent of the filaments. This phenomenon can be modeled by assuming that at some distance behind the wing all vortex lines connect with the vortex line of maximum intensity (nose vortex) into two vortex filaments, whose intensity equals the sum of the intensities of the coalescing vortex lines. These vortex filaments obey the laws governing the behavior of free vortex lines: they align along the stream lines. At some distance from the point of coalescence of all vortex lines into a filament (focus), the action of the vortices connected to

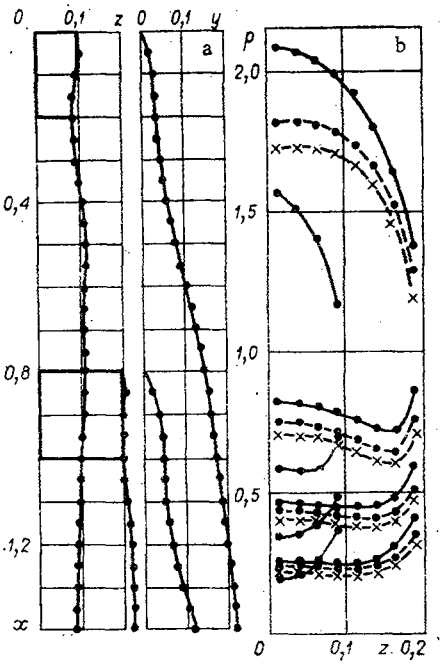

Fig. 5

the wing and the part of the free vortex lines before focusing becomes weaker and the filaments begin to interact with one another according to the law of interaction of two infinite lines (interaction of two point vortices [8]); the vortices descend.

For the wing with $\lambda = 2$, at an angle of attack $\alpha = 15°$ with $N_x \times N_z = 8 \times 8$, and $\varepsilon = 0.05\%$, when the point at which the vortices are focused is chosen along one of the chords behind the wing ($x_f = 2$), the behavior and intensity of the free vortex lines up to the section $x \leqslant 1.5$ in the case of focusing differs little from the calculations using the vortex sheet scheme. Almost immediately after focusing, the vortex filaments become rectilinear. The projection of a vortex filament on the plane $y = 0$ coincides with the line $z = 1.1$ (the line $z = 1.0$ is the line of the lateral edge of the wing), and the vortex filaments practically do not diverge after focusing. The projection of a vortex filament in the plane $z = 0$ soon after focusing (beginning with $x \approx 2.5$) becomes a straight line with a slope less than the slope of the velocity of the unperturbed flow ($\tan\alpha = 0.268$; $\tan\theta = 0.225$). The descent, according to the numerical calculations performed, constitutes 2°20'.

An equation is presented in [8] for the rate of descent of two rectilinear vortex lines with identical intensity $v_y = \Gamma/2\pi l$, where Γ is the intensity of each of the vortices and l is the distance between them. According to this equation, the descent of the computed vortex filaments can be computed assuming they are infinite straight lines. If the intensity of the filament is $\Gamma = 0.490$ and the distance between then is $l = 2 \cdot 1.1 = 2.2$, then $v_y = 0.0352$. The orientation of the vortex filament is determined by the equation

$$\operatorname{tg}\theta = dy/dx = (U_\infty \sin\alpha - v_y \cos\alpha)/(U_\infty \cos\alpha + v_y \sin\alpha),$$

from which it follows that $\tan\theta = 0.220$. The descent, according to this estimate, is $\approx 2°35'$.

The rolling up of the vortex sheet into filaments has little effect on the aerodynamic characteristics of the wing itself, but it can have an appreciable effect on the carrying surfaces, situated in the wake behind the wing.

We performed calculations of flow at an angle of attack $\alpha = 15°$ for a tendem configuration of wings $\lambda = 1$, $\lambda = 2$ with identical chords and situated in the same plane one behind the other at a distance of three chords, using the vortex sheet scheme and the filament scheme. The unit of length in the case of the tandem was chosen as the distance from the front edge of the first wing to the rear edge of the second wing. The length of the chord of the wings in this case equals 0.2; the distance between the rear edge of the first wing and the front edge of the rear wing is 0.6. In the vortex sheet scheme, the free vortex lines line up for both wings up to the section $x_\infty = 1.4$ and then they proceed as infinite straight lines forming a slope $\alpha = 15°$ with the x axis. In the vortex filament scheme, the free

vortex lines of the first wing are focused at a distance of one chord behind the rear edge of the first wing ($x_{f_1} = 0.4$), and then these vortex lines proceed in the form of a filament, which conforms to the laws of a free vortex line under the action of the entire vortex system of the tandems. The free vortex lines of the second wing are focused at a distance of one chord behind the rear edge of the second wing ($x_{f_2} = 1.2$) and then these vortex lines proceed as a filament, whose position is likewise established under the action of the entire vortex system of the tandem.

Figure 5a shows the behavior of vortex lines in the filament scheme: the coordinates of the nose vortex line of the first wing on the section $0 \leqslant x \leqslant 0.4$, which in the section $0.4 \leqslant x \leqslant 1.4$ coalesces into the vortex filament of the first wing, and the coordinates of the nose vortex line of the second wing on the section $0.8 \leqslant x \leqslant 1.2$, which on the section $1.2 \leqslant x \leqslant 1.4$ coalesces into the vortex filament of the second wing. In the filament scheme, there is a larger change in the trajectory of the first vortex filament in the zone of the second wing as compared to the trajectory of this filament for an isolated wing and there is an appreciable change in the trajectory of the nose vortex of the second wing and in the vortex filament of the second wing continuing it.

The change in the vortex structures above the second wing leads to a change in the pressure distribution on this wing. Figure 5b shows the load distribution in four sections x = const, passing through points on the second wing at which the impenetrability condition is satisfied, for the vortex sheet scheme (dashed lines with points) and for the filament scheme (dashed lines with cross marks). For comparison, the continuous lines in the figure show the load distribution in the same four sections on an isolated wing $\lambda = 2$ and on four sections of the wing $\lambda = 1$. The load distribution on the wing $\lambda = 1$ remains practically unchanged when the wing $\lambda = 2$ is placed in its wake at a distance of three chords: it is identical for the isolated wing and for the wing in a tandem system both in the vortex sheet scheme and in the vortex filament scheme. The load distribution on the wing $\lambda = 2$, located in the wake of the wing $\lambda = 1$, changes appreciably. For the vortex sheet scheme, the load on the wing $\lambda = 2$ under the rolled up vortex sheet of the first wing decreases. In the vortex filament scheme, the vortex filament of the first wing, which is located much lower than the nose vortex line of the first wing in the vortex sheet scheme and gives rise to a larger decrease in load on the wing $\lambda = 2$, passes above the wing $\lambda = 2$. The difference in the load distribution on the wing $\lambda = 2$, located in the wake of the wing $\lambda = 1$, according to these two schemes is appreciable: the quantity C_n for the tandem differs by 4%.

We thank S. D. Ermolenko and Yu. A. Rogozin, who provided detailed information on the experimental results obtained in [7].

LITERATURE CITED

1. V. V. Golubev, Lectures on the Theory of Wings [in Russian], Gostekhizdat, Moscow (1949).
2. A. A. Nikol'skii, "Second form of motion of an ideal fluid near a circumfluous body (investigation of detached flows)," Dokl. Akad. Nauk SSSR, 116, No. 3 (1957).
3. S. M. Belotserkovskii, "Calculation of flow past wings with arbitrary shape in the plane over a wide range of angles of attack," Izv. Akad. Nauk SSSR, Mekh. Zhidk. Gaza, No. 4 (1968).
4. N. F. Vorob'ev and G. N. Shashkina, "Problem of selecting a discrete vortex scheme of a wing," in: Problems of Flow Past Bodies with Three-Dimensional Configuration [in Russian], Izd. ITPM Sib. Otd. Akad. Nauk SSSR, Novosibirsk (1978).
5. G. N. Shashkina and N. F. Vorob'ev, "Modeling conditions of vortex sheet detachment in calculating flow past a wing using a discrete vortex scheme," ChMMSS, 10, No. 3 (1979).
6. S. M. Belotserkovskii and M. I. Nisht, Detached and Undetached Ideal Fluid Flow Past Thin Wings [in Russian], Nauka, Moscow (1978).
7. S. D. Ermolenko, Yu. A. Rogozin, et al., "Modeling of aircraft by a thin flat surface having the shape of the projection of the aircraft in the plane," Uch. Zap. TsAGI, 10, No. 2 (1979).
8. N. E. Kochin, I. A. Kibel', and N. V. Roze, Theoretical Hydrodynamics [in Russian], Part 1, Fizmatgiz, Moscow (1963).